International Journal of Pure and Applied Mathematics
Volume 50 No. 2 2009, 259-267

THE EFFECT OF PRESSURE RELAXATION IN TWO-PHASE FLOW CALCULATIONS

Svend Tollak Munkejord
Department of Energy Processes
SINTEF Energy Research
11, Sem Sælands Veg, Trondheim, NO-7465, NORWAY
e-mail: stm@pvv.org

Abstract: This paper analyses the approach of using a two-pressure two-fluid model with instantaneous pressure relaxation, comparing it to the more traditional approach of using a single-pressure two-fluid model. To do that, the multi-stage centred (MUSTA) scheme for non-conservative two-fluid models of Munkejord, Evje and Flåtten [8] is applied to and tested for the two-pressure two-fluid model.

Within this framework, example calculations show that from a modelling point of view, using the two-pressure two-fluid model with instantaneous pressure relaxation is not different from using the single-pressure two-fluid model. From a computational point of view, however, the former approach has the significant disadvantage of introducing a large amount of numerical smearing.

AMS Subject Classification: 76T10, 76M12, 65M12, 35L65
Key Words: two-phase flow, two-fluid model, MUSTA scheme, pressure

1. Model Formulation

This work considers only the essential parts of the two-fluid model, to enable a comparison between a solution approach with, and one without, pressure relaxation.

Received: August 14, 2008

1.1. Four-Equation System

Consider a model consisting of a mass-conservation equation and a momentum-balance equation for each phase, k:

$$\frac{\partial}{\partial t}(\alpha_k\rho_k) + \frac{\partial}{\partial x}(\alpha_k\rho_k v_k) = 0, \tag{1}$$

$$\frac{\partial}{\partial t}(\alpha_k\rho_k v_k) + \frac{\partial}{\partial x}\left(\alpha_k\rho_k v_k^2\right) + \alpha_k\frac{\partial p}{\partial x} + \Delta p_\mathrm{i}\frac{\partial \alpha_k}{\partial x} = \alpha_k\rho_k g_x + m_{\mathrm{i}k}. \tag{2}$$

For $k \in \{\mathrm{g}, \ell\}$ (gas and liquid), ρ_k denotes the density, v_k the velocity, α_k the volume fraction, g_x the gravitational acceleration in x direction, and p the common pressure. $\Delta p_\mathrm{i} = p - p_\mathrm{i}$ is the interfacial pressure difference and $m_{\mathrm{i}k}$ is the interfacial momentum exchange; here we consider friction.

The volume fractions satisfy $\alpha_\mathrm{g} + \alpha_\ell = 1$. The equation of state

$$p = p_k(\rho_k) = c_k^2(\rho_k - \rho_k^\circ) \tag{3}$$

is employed, where the speed of sound, c_k, and the 'reference density', ρ_k° are constants for each phase, constituting an assumption of constant entropy or temperature.

1.2. Five-Equation System

In [11], the two-fluid model was augmented with an advection equation for the volume fraction – with an added pressure-relaxation term. Here we do likewise, except that in the present case, the energy equation is disregarded for simplicity. The model then reads:

$$\frac{\partial \alpha_\mathrm{g}}{\partial t} + v_\mathrm{i}\frac{\partial \alpha_\mathrm{g}}{\partial x} = r_p(p_\mathrm{g} - p_\ell), \tag{4}$$

$$\frac{\partial}{\partial t}(\alpha_k\rho_k) + \frac{\partial}{\partial x}(\alpha_k\rho_k v_k) = 0, \tag{5}$$

$$\frac{\partial}{\partial t}(\alpha_k\rho_k v_k) + \frac{\partial}{\partial x}\left(\alpha_k\rho_k v_k^2\right) + \alpha_k\frac{\partial p_k}{\partial x} + \Delta p_{\mathrm{i}k}\frac{\partial \alpha_k}{\partial x} = \alpha_k\rho_k g_x + m_{\mathrm{i}k}, \tag{6}$$

for $k \in \{\mathrm{g}, \ell\}$. Herein, r_p is a pressure-relaxation parameter, and v_i is the average interfacial velocity, to be defined in the following. It is also possible to consider a large interfacial friction, or *velocity relaxation* in the current jargon. Here, however, $m_{\mathrm{i}k}$ remains relatively small. We employ the same equation of state as for the four-equation system, but now, the pressures in each phase are independent:

$$p_k = p_k(\rho_k) = c_k^2(\rho_k - \rho_k^\circ). \tag{7}$$

The equation-system matrix of the five-equation system is diagonalizable with real eigenvalues almost everywhere, except at the sonic points (see e.g. [10]). Further, simple, analytical expressions are available for the eigenvalues and eigenvectors. More details are also given in [6] for the current context. These are advantages for the five-equation system compared to the four-equation system, where analytical expressions for the eigenstructure are only available for particular choices for the constitutive relations, and for which there are regions where the hyperbolicity is lost.

1.2.1. Overview of the Solution Procedure

The relaxation term may become large. Therefore, the equation system (4)–(6) is split in two, and solved using a fractional-step technique. The hyperbolic part of the system is (4)–(6) with $r_p \equiv 0$. The remainder is the relaxation part:

$$\frac{\partial \alpha_{\mathrm{g}}}{\partial t} = r_p(p_{\mathrm{g}} - p_\ell), \quad \frac{\partial}{\partial t}(\alpha_k \rho_k) = 0, \quad \frac{\partial}{\partial t}(\alpha_k \rho_k v_k) = 0. \tag{8}$$

Let $\boldsymbol{q}_j^n$ denote the numerical approximation to the cell average of the vector of unknowns $\boldsymbol{q}(x, t_n)$ in control volume j at time step n. With $\boldsymbol{q}_j^n$ as an initial value, the solution at the next time step, $\boldsymbol{q}_j^{n+1}$, can be found as follows:

1. Find $\boldsymbol{q}_j^*$ as the solution of the hyperbolic part of (4)–(6) at t_{n+1}.

2. Find $\boldsymbol{q}_j^n$ as the solution of the relaxation system (8) at t_{n+1} with $\boldsymbol{q}_j^*$ as initial value.

For step 1, the MUSTA scheme will be employed. For step 2, a numerical solver for ordinary differential equations can be used for finite-rate relaxation. For infinite/instantaneous relaxation, it is more efficient to employ a dedicated procedure solving a second-degree equation.

It should be emphasized that for instantaneous pressure relaxation, the volume-fraction advection equation (4) becomes singular, and the two phasic pressures become equal. Hence it is expected that the equation system reduces to the four-equation system.

1.2.2. Interface Velocity

Following [11], we will use the mass-weighted velocity as a model for the average interfacial velocity in (4):

$$v_{\mathrm{i}} = \frac{\alpha_{\mathrm{g}} \rho_{\mathrm{g}} v_{\mathrm{g}} + \alpha_\ell \rho_\ell v_\ell}{\alpha_{\mathrm{g}} \rho_{\mathrm{g}} + \alpha_\ell \rho_\ell}. \tag{9}$$

1.3. Interfacial-Pressure Model

Both in the four-equation and the five-equation system, a model is needed for the interfacial pressure difference. In this work, the model of [1] is employed:

$$p_k - p_{\mathrm{i}k} = \Delta p_{\mathrm{i}k} = \delta \frac{\alpha_{\mathrm{g}}\alpha_\ell\rho_{\mathrm{g}}\rho_\ell}{\alpha_{\mathrm{g}}\rho_\ell + \alpha_\ell\rho_{\mathrm{g}}}(v_{\mathrm{g}} - v_\ell)^2. \tag{10}$$

The main justification of the expression is to render the four-equation system hyperbolic for a reasonable range of parameters [1]. Like [4], we take $\delta = 1.2$.

1.4. Canonical Form of the Equation Systems

Both two-fluid models of the preceding subsections can be written in the following form:

$$\frac{\partial \boldsymbol{q}}{\partial t} + \frac{\partial \boldsymbol{f}(\boldsymbol{q})}{\partial x} + \boldsymbol{B}(\boldsymbol{q})\frac{\partial \boldsymbol{w}(\boldsymbol{q})}{\partial x} = \boldsymbol{s}(\boldsymbol{q}). \tag{11}$$

The model of Section 1.2 can be expressed with

$$\boldsymbol{q} = \begin{bmatrix} \alpha_{\mathrm{g}} \\ \alpha_{\mathrm{g}}\rho_{\mathrm{g}} \\ \alpha_\ell\rho_\ell \\ \alpha_{\mathrm{g}}\rho_{\mathrm{g}}v_{\mathrm{g}} \\ \alpha_\ell\rho_\ell v_\ell \end{bmatrix}, \quad \boldsymbol{f}(\boldsymbol{q}) = \begin{bmatrix} 0 \\ \alpha_{\mathrm{g}}\rho_{\mathrm{g}}v_{\mathrm{g}} \\ \alpha_\ell\rho_\ell v_\ell \\ \alpha_{\mathrm{g}}\rho_{\mathrm{g}}v_{\mathrm{g}}^2 + \alpha_{\mathrm{g}}\Delta p_{\mathrm{i}} \\ \alpha_\ell\rho_\ell v_\ell^2 + \alpha_\ell\Delta p_{\mathrm{i}} \end{bmatrix}, \quad \boldsymbol{s}(\boldsymbol{q}) = \begin{bmatrix} r_p(p_{\mathrm{g}} - p_\ell) \\ 0 \\ 0 \\ \alpha_{\mathrm{g}}\rho_{\mathrm{g}}g_x + m_{\mathrm{ig}} \\ \alpha_\ell\rho_\ell g_x + m_{\mathrm{i}\ell} \end{bmatrix}, \tag{12}$$

and

$$\boldsymbol{B}(\boldsymbol{q}) = \begin{bmatrix} v_{\mathrm{i}} & 0 & 0 & 0 & 0 \\ 0 & 0 & 0 & 0 & 0 \\ 0 & 0 & 0 & 0 & 0 \\ 0 & 0 & 0 & \alpha_{\mathrm{g}} & 0 \\ 0 & 0 & 0 & 0 & \alpha_\ell \end{bmatrix}, \quad \boldsymbol{w}(\boldsymbol{q}) = \begin{bmatrix} \alpha_{\mathrm{g}} \\ 0 \\ 0 \\ p_{\mathrm{g}} - \Delta p_{\mathrm{ig}} \\ p_\ell - \Delta p_{\mathrm{i}\ell} \end{bmatrix}. \tag{13}$$

The expressions for the model of Section 1.1 are analogous.

2. The MUSTA Scheme

A MUSTA scheme was derived for the four-equation system in [8] by using the framework of path-conservative schemes of [9]. With the canonical form of the equation system given above, the scheme can be applied rather directly to the five-equation system. The main building blocks in the MUSTA scheme will be recalled here for convenience.

2.1. Building Blocks

Consider the equation system (11) with $\boldsymbol{s} = \boldsymbol{0}$. It can be discretized as

$$\frac{\boldsymbol{q}_j^{n+1} - \boldsymbol{q}_j^n}{\Delta t} + \frac{\boldsymbol{f}_{j+1/2} - \boldsymbol{f}_{j-1/2}}{\Delta x} + \frac{\boldsymbol{d}_{j-1/2}^{+} + \boldsymbol{d}_{j+1/2}^{-}}{\Delta x} = \boldsymbol{0}, \tag{14}$$

with

$$\boldsymbol{d}_{j+1/2}^{+} = \boldsymbol{B}_{j+1/2}\big(\boldsymbol{w}_{j+1} - \boldsymbol{w}_{j+1/2}\big) \text{ and } \boldsymbol{d}_{j+1/2}^{-} = \boldsymbol{B}_{j+1/2}\big(\boldsymbol{w}_{j+1/2} - \boldsymbol{w}_j\big). \tag{15}$$

2.1.1. The FORCE Scheme

The basic building block of MUSTA is the first-order centred (FORCE) scheme of [13]. The FORCE numerical flux is defined as the arithmetic mean of the Lax–Friedrichs flux and the Richtmyer Lax–Wendroff flux:

$$\boldsymbol{f}_{j+1/2}^{\mathrm{FORCE}} = \frac{1}{2}\Big(\boldsymbol{f}_{j+1/2}^{\mathrm{LF}} + \boldsymbol{f}_{j+1/2}^{\mathrm{LW}}\Big). \tag{16}$$

It is then natural to assume the same averaging for the cell-interface value of the non-conservative variables vector, $\boldsymbol{w}_{j+1/2}$:

$$\boldsymbol{w}_{j+1/2}^{\mathrm{FORCE}} = \frac{1}{2}\Big(\boldsymbol{w}_{j+1/2}^{\mathrm{LF}} + \boldsymbol{w}_{j+1/2}^{\mathrm{LW}}\Big). \tag{17}$$

2.1.2. The Lax–Friedrichs Scheme

For the non-conservative system (11), De Vugst [3] proposed the Lax–Friedrichs discretization

$$\boldsymbol{f}_{j+1/2}^{\mathrm{LF}} = \frac{1}{2}\big(\boldsymbol{f}(\boldsymbol{q}_j) + \boldsymbol{f}(\boldsymbol{q}_{j+1})\big) + \frac{1}{2}\frac{\Delta x}{\Delta t}(\boldsymbol{q}_j - \boldsymbol{q}_{j+1}), \tag{18}$$

with

$$\boldsymbol{d}_{j+1/2}^{\pm} = \frac{1}{2}\boldsymbol{B}_{j+1/2}(\boldsymbol{w}_{j+1} - \boldsymbol{w}_j). \tag{19}$$

2.1.3. The Richtmyer Scheme

It is the two-step Richtmyer version of the Lax–Wendroff scheme that is employed in the FORCE scheme. First, the cell-interface solution is evolved one half time step using a simple Lax–Friedrichs scheme:

$$\boldsymbol{q}_{j+1/2}^{n+1/2} = \frac{1}{2}\Big(\boldsymbol{q}_j^n + \boldsymbol{q}_{j+1}^{n+1/2}\Big) - \frac{1}{2}\frac{\Delta t}{\Delta x}\Big(\boldsymbol{f}\big(\boldsymbol{q}_{j+1}^n\big) - \boldsymbol{f}\big(\boldsymbol{q}_j^n\big)\Big)$$

$$- \frac{1}{2}\frac{\Delta t}{\Delta x}\boldsymbol{B}^n_{j+1/2}\Big(\boldsymbol{w}^n_{j+1} - \boldsymbol{w}^n_j\Big). \quad (20)$$

Then the numerical cell-interface values to be used in (16) and (17) are given as:

$$\boldsymbol{f}^{\mathrm{LW}}_{j+1/2} = \boldsymbol{f}\big(\boldsymbol{q}^{n+1/2}_{j+1/2}\big), \qquad \boldsymbol{w}^{\mathrm{LW}}_{j+1/2} = \boldsymbol{w}\big(\boldsymbol{q}^{n+1/2}_{j+1/2}\big). \quad (21)$$

2.1.4. The Cell-Interface Matrix

As shown in [8], a path-conservative scheme can be achieved by calculating the cell-interface matrix, $\boldsymbol{B}_{j+1/2}$, from an arithmetic average of the states of the cells j and $j+1$.

2.2. Algorithm

The MUSTA procedure employed here is similar to the previous ones for the Euler equations [12] and for the drift-flux model [7], but it is extended to account for the non-conservative terms in the governing equations. For calculating the numerical flux, $\boldsymbol{f}_{j+1/2}$, and the non-conservative variables vector, $\boldsymbol{w}_{j+1/2}$, the Riemann problem at the cell interface, $x_{j+1/2}$, is transformed to a local grid:

$$\frac{\partial \boldsymbol{q}}{\partial t} + \frac{\partial \boldsymbol{f}(\boldsymbol{q})}{\partial \xi} + \boldsymbol{B}(\boldsymbol{q})\frac{\partial \boldsymbol{w}(\boldsymbol{q})}{\partial \xi} = \boldsymbol{0}, \qquad \boldsymbol{q}(\xi, 0) = \begin{cases} \boldsymbol{q}_j = \boldsymbol{q}_{\mathrm{L}} & \text{if } \xi < 0, \\ \boldsymbol{q}_{j+1} = \boldsymbol{q}_{\mathrm{R}} & \text{if } \xi \geq 0, \end{cases} \quad (22)$$

where the position $\xi = 0$ corresponds to $x_{j+1/2}$. This local Riemann problem is then solved approximately by employing the FORCE scheme, where the local grid is indexed by n:

$$\frac{\boldsymbol{q}^{m+1}_n - \boldsymbol{q}^m_n}{\Delta t_{\mathrm{loc}}} + \frac{\boldsymbol{f}^{\mathrm{FORCE}}_{n+1/2} - \boldsymbol{f}^{\mathrm{FORCE}}_{n-1/2}}{\Delta x} + \frac{\boldsymbol{B}_{n-1/2}(\boldsymbol{w}_n - \boldsymbol{w}^{\mathrm{FORCE}}_{n-1/2}) + \boldsymbol{B}_{n+1/2}(\boldsymbol{w}^{\mathrm{FORCE}}_{n+1/2} - \boldsymbol{w}_n)}{\Delta x} = \boldsymbol{0}. \quad (23)$$

Herein, $\boldsymbol{f}^{\mathrm{FORCE}}_{n+1/2}$, $\boldsymbol{w}^{\mathrm{FORCE}}_{n+1/2}$ and $\boldsymbol{B}_{n+1/2} = \boldsymbol{B}(\boldsymbol{q}_n, \boldsymbol{q}_{n+1})$ are calculated as described in the preceding subsections, while $\boldsymbol{w}_n = \boldsymbol{w}(\boldsymbol{q}_n)$. The local pseudo-time step, Δt_{loc}, is calculated using a CFL number of 0.9 on the local grid. For the four-equation system, the maximum eigenvalues are approximated using the estimates of [4].

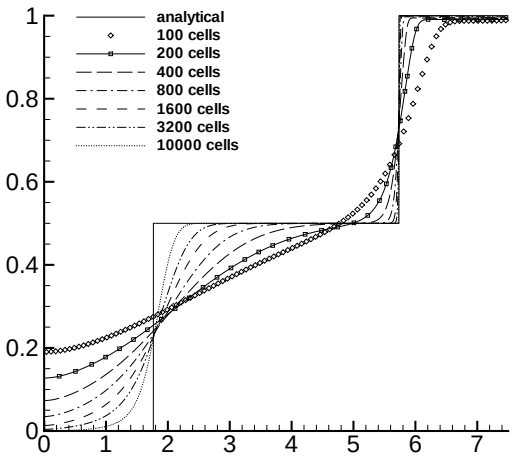

Figure 1: Four-equations system (no relaxation). Liquid volume fraction. Effect of pressure relaxation.

3. Results and Conclusion

Here the water-air separation problem introduced by [2] is considered. It consists of a vertical tube of length $L = 7.5\,\mathrm{m}$, closed at both ends. Initially it has a uniform pressure of $p = 1 \times 10^5\,\mathrm{Pa}$ and a volume fraction of $\alpha_\ell = 0.5$. At time $t = 0$, the phases start separating under the influence of gravity. To avoid very large velocity differences, an interfacial friction model similar to the one employed in [5] is introduced. Even so, this problem poses a great challenge regarding the robustness of the scheme.

Calculations have been performed using the MUSTA_{2-2} scheme with a CFL number of 0.3. In the equation of state, the parameters $c_\mathrm{g} = \sqrt{10^5}\,\mathrm{m/s}$, $c_\ell = 1000\,\mathrm{m/s}$, $\rho_\mathrm{g}^\circ = 0$ and $\rho_\ell^\circ = 999.9\,\mathrm{kg/m^3}$ were taken. Liquid volume fractions calculated at $t = 0.6\,\mathrm{s}$ are shown in Figure 1 and Figure 2. Both the profiles in Figure 1 calculated employing the four-equation system and those in Figure 2 calculated using the five-equation system with instantaneous pressure relaxation, approach the same solution with grid refinement. However, the latter profiles are significantly more smeared than the former. Since the numerical methods are otherwise analogous, we can conclude that the smearing is introduced by the pressure relaxation.

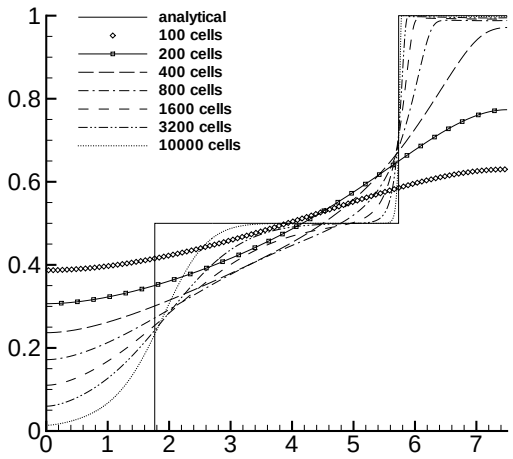

Figure 2: Four-equations system (instant relaxation). Liquid volume fraction. Effect of pressure relaxation.

Acknowledgements

This work was financed by SINTEF Energy Research and the Research Council of Norway. Thanks are due to T. Flåtten at the Institute for Energy Technology (IFE) for the fruitful discussions. K.E. Teigen at the Norwegian University of Science and Technology (NTNU) has read and commented the manuscript.

References

[1] D. Bestion, The physical closure laws in the CATHARE code, *Nucl. Eng. Design*, **124** (1990), 229-245.

[2] F. Coquel, K. El Amine, E. Godlewski, B. Perthame, P. Rascle, A numerical method using upwind schemes for the resolution of two-phase flows, *J. Comput. Phys.*, **136** (1997), 272-288.

[3] F. De Vuyst, Stable and accurate finite volume method based on pure convexity arguments for hyperbolic systems of conservation law, *J. Comput. Phys.*, **193** (2004), 426-468.

[4] S. Evje, T. Flåtten, Hybrid flux-splitting schemes for a common two-fluid model, *J. Comput. Phys.*, **192** (2003), 175-210.

[5] S. Evje, T. Flåtten, Weakly implicit numerical schemes for a two-fluid model, *SIAM J. Sci. Comput.*, **26** (2005), 1449-1484.

[6] S.T. Munkejord, Comparison of Roe-type methods for solving the two-fluid model with and without pressure relaxation, *Comput. Fluids*, **36** (2007), 1061-1080.

[7] S.T. Munkejord, S. Evje, T. Flåtten, The multi-stage centred-scheme approach applied to a drift-flux two-phase flow model, *Int. J. Numer. Meth. Fl.*, **52** (2006), 679-705.

[8] S.T. Munkejord, S. Evje, T. Flåtten, A MUSTA scheme for a non-conservative two-fluid model, *Submitted for publication*.

[9] C. Pars, Numerical methods for nonconservative hyperbolic systems: A theoretical framework, *SIAM J. Numer. Anal.*, **44** (2006), 300-321.

[10] V.H. Ransom, D.L. Hicks, Hyperbolic two-pressure models for two-phase flow, *J. Comput. Phys.*, **53** (1984), 124-151.

[11] R. Saurel, R. Abgrall, A multiphase Godunov method for compressible multifluid and multiphase flow, *J. Comput. Phys.*, **150** (1999), 425-467.

[12] V.A. Titarev, E.F. Toro, MUSTA schemes for multi-dimensional hyperbolic systems: analysis and improvements, *Int. J. Numer. Meth. Fl.*, **49** (2005), 117-147.

[13] E.F. Toro, *Riemann Solvers and Numerical Methods for Fluid Dynamics*, Springer-Verlag, Berlin, second edn. (1999), ISBN 3-540-65966-8.